

## Contents

<b>Case 1</b>	<b>Choroidal Melanoma</b> . . . . .	24
<b>Case 2</b>	<b>Grave's Ophthalmopathy</b> . . . . .	26
<b>Case 3</b>	<b>Inflammatory Pseudotumor of the Orbit</b> . . . . .	28
<b>Case 4</b>	<b>Orbital Hemangioma</b> . . . . .	30
<b>Case 5</b>	<b>Orbital Lymphoma</b> . . . . .	32
<b>Case 6</b>	<b>Optic Nerve Sheath Meningioma</b> . . . . .	34
<b>Case 7</b>	<b>Craniopharyngioma</b> . . . . .	36
<b>Case 8</b>	<b>Hypothalamic Hamartoma</b> . . . . .	38
<b>Case 9</b>	<b>Pituitary Adenoma</b> . . . . .	40
<b>Case 10</b>	<b>Rathke's Cleft Cyst</b> . . . . .	42

**Case 1****Choroidal  
Melanoma****History**

A 51-year-old man presented with a several-month history of progressive visual loss in the right eye. On ophthalmologic examination, an intraocular mass was found.

**Comments**

Malignant melanomas are the most common primary intraocular tumors in adults. Nevertheless, these lesions are infrequent. The tumor arises from melanocytes within the choroid. Choroidal melanoma have race predominance, and most often affect white people while incidence among blacks is extremely rare. Median age is 55 years. Choroidal melanomas may have variable coloration, ranging from amelanotic to darkly pigmented, and are typically circumscribed, domed-shaped masses that grow to the vitreous cavity. Choroidal melanoma may metastasize before diagnosis. The tumor can spread hematogenously to the liver, lung, bone, skin, and the central nervous system (CNS).

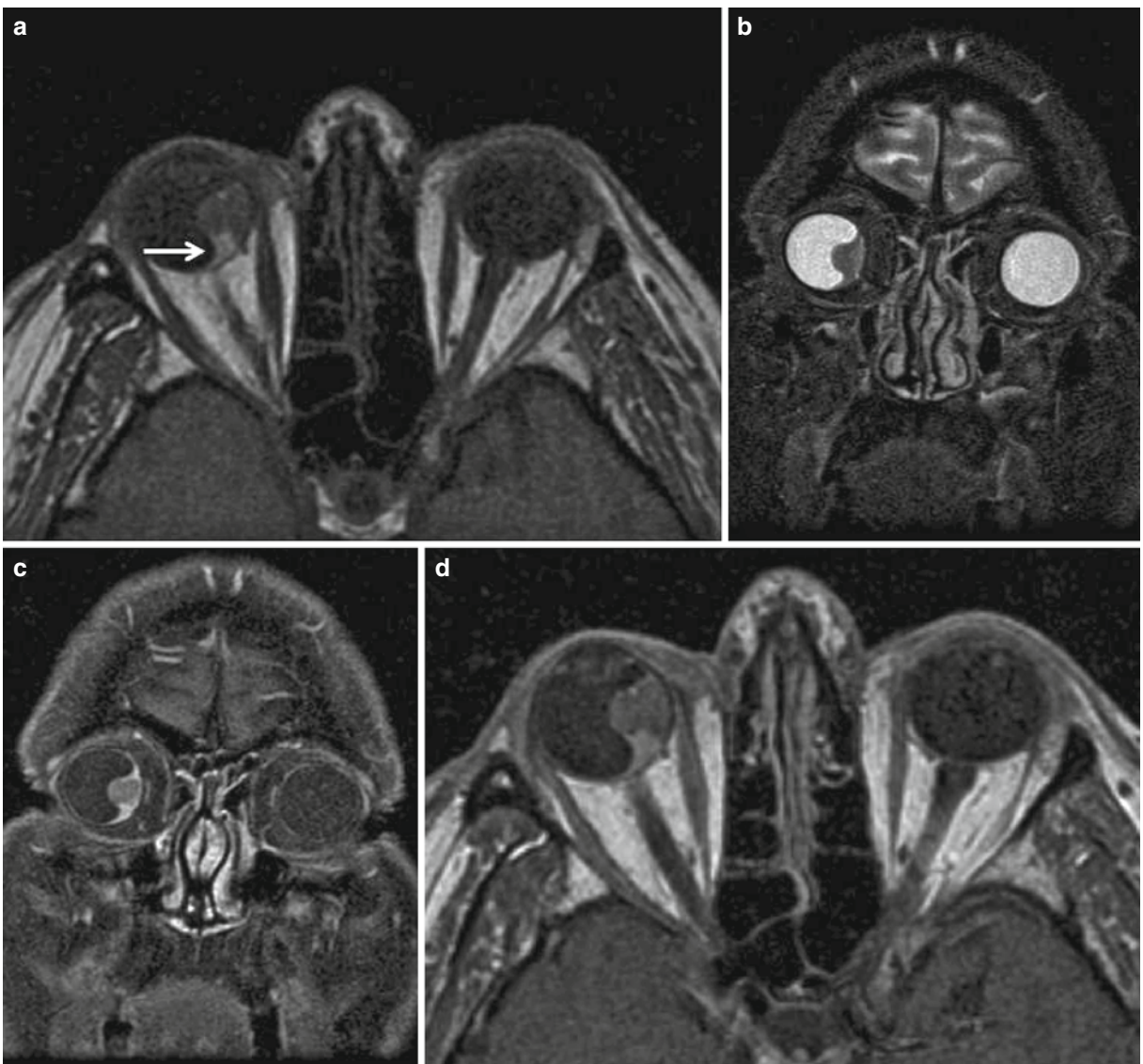


**Fig. 2.1**

Choroidal melanomas usually remain asymptomatic for long time and the diagnosis is made incidentally during a routine ophthalmologic examination. In general, the more anterior their origin, the longer the delay of any symptoms. As the tumor grows, it may become symptomatic. The most common clinical presentation is painless visual loss with decreased visual acuity and visual field defects.

Because of their anatomic location, choroidal tumors are not accessible to biopsy without intraocular surgery. Consequently, the diagnosis must be made on the basis of clinical examination in conjunction with different diagnostic modalities such as ultrasound, computed tomography (CT), magnetic resonance imaging (MRI), and angiography. Lesions more than 3 mm in size are usually well detected on CT and MRI, whereas smaller lesions are better evaluated with ultrasound. The accurate technique to diagnose the tumor and to determine its size is ultrasound. On B-scan mode, intraocular melanoma appears as a rounded or mushroom-shaped hypoechoic mass that produces excavation of underlying uveal tissue and shadowing of subjacent soft tissues. A thin hyperechoic rim is sometimes seen and represents a combination of elevated retina and peripheral blood vessels. These tumors are very vascular lesions. Color Doppler ultrasound allows evaluating the tumor vascularization both internally and in the periphery. This tumor characteristic is useful to differentiate choroidal melanoma from other non-neoplastic entities such as subretinal hemorrhage. Ultrasound may also detect some complications of the tumor as retinal elevation and vitreous hemorrhage. CT scan is more useful than ultrasound to evaluate extraocular extension and may help differentiate between choroidal or retinal detachment and a solid tumor. After contrast material administration, choroidal melanoma shows moderate enhancement. CT scan also is sensitive in detecting calcium, a feature of some tumors different from uveal melanomas (characteristically choroidal osteoma). On MRI, most choroidal melanomas appear as areas of high signal intensity on T1- and proton density-weighted MR images, due to the paramagnetic property of melanin, and moderately low signal intensity on T2-WI. The tumor demonstrates moderate enhancement after intravenous gadolinium injection.

Documented growth of a lesion on serial examinations is the most important clinical feature favoring the diagnosis of a choroidal melanoma. Differential diagnosis must be made with retinal detachment, choroidal detachment, choroidal metastasis, choroidal hemangioma, and large choroidal nevus.

Treatment depends on several factors such as visual acuity, size of tumor, age of the patient, and presence of metastases. Small tumors can be managed by periodic observation. In cases of tumor growth and in large and/or complicated tumors which compromise visual function, enucleation is indicated. Nevertheless, enucleation does not prevent metastasis.

MRI study demonstrates a lobulated mass located in nasal aspect of the right ocular globe. The lesion appears slightly hyperintense to vitreous humor on axial T1-weighted image (Fig. 2.1a) and hypointense on coronal STIR sequence (Fig. 2.1b). A hyperintense rim surrounded the mass can be seen on T1-WI, which represents a retinal detachment (*arrow* in Fig. 2.1a). Contrast-enhanced fat-saturation T1-weighted image (Fig. 2.1c) and contrast-enhanced spin-echo T1-WI (Fig. 2.1d) show homogeneous enhancement of the lesion.

## Imaging Findings

**Case 2****Grave's Ophthalmopathy****History**

A 57-year-old man presented with bilateral exophthalmos and eyelid swelling. On ophthalmologic examination, diplopia, visual acuity loss on the right eye, and right papilledema were found.

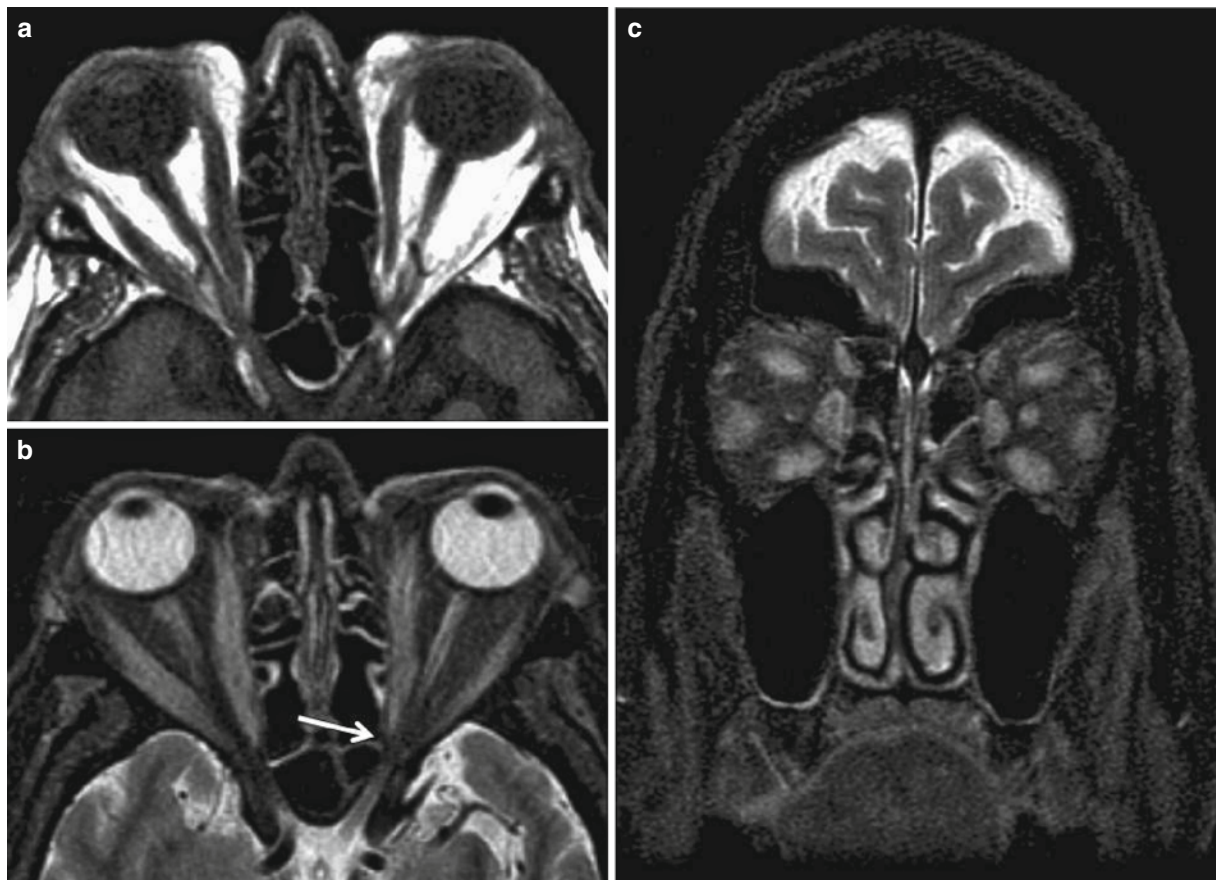


**Fig. 2.2**

## Comments

Grave's ophthalmopathy (GO) is a thyroid-associated orbitopathy that represents a part of Grave's disease, an autoimmune process that can affect the orbital and periorbital tissue, the thyroid gland, and, rarely, the pretibial skin or digits (thyroid acropachy). Eye involvement in Grave's disease is clinically evident in 25–50% of patients. GO may precede, coincide, or follow the systemic complications of dysthyroidism. The underlying pathophysiology of GO is thought to be an antibody-mediated reaction against the TSH receptors present in retrobulbar tissue. There is a lymphocytic infiltration of the orbital tissue that causes edema in the extraocular muscles and transformation of preadipocyte fibroblasts into adipocytes. The enlargement of extraocular muscles in conjunction with the orbital fat accumulation produce an increase in orbital volume causing exophthalmos and, occasionally, optic nerve compression at the narrow posterior apex of the orbit. The edema results in tissue damage and fibrosis, with restriction in extraocular motility and lagophthalmos. GO is the most common cause of unilateral and bilateral proptosis in adults. GO usually occurs in patients aged 30–50 years and is much more common in females, although severe cases occur more often in males.

The ocular manifestations of GO include eyelid swelling or retraction, chemosis, tearing, corneal erosions or ulcerations, abnormal eye motility, exophthalmos, and periorbital edema. Although most cases of GO do not result in visual loss, GO can cause vision-threatening exposure keratopathy, troublesome diplopia, and compressive optic neuropathy.

In typical cases, the diagnosis can be established clinically and imaging studies are not necessary. Orbital imaging is recommended in cases of very asymmetrical clinical picture and in cases of clinical suspicion of optic nerve involvement. Imaging techniques include ultrasound, CT, and MRI. Orbital ultrasound can quickly confirm if the patient has thickened muscles or an enlarged superior ophthalmic vein. CT and MRI, with both axial and coronal views, usually reveal thick muscles with tendon sparing. The inferior rectus muscle and the medial rectus muscle are usually involved. Bilateral muscle enlargement is common; unilateral cases usually represent asymmetric involvement rather than normality of the less involved side. The superior ophthalmic vein may be dilated. CT scan provides excellent views of the bony anatomy of the orbit, which is important in cases that orbital decompression is required. MRI is better to evaluate the orbital contents including the optic nerve, orbital fat, and extraocular muscles.

Regarding treatment, the main goal is to achieve and maintain a euthyroid state. These measures alone are sufficient in many cases, because the majority of patients with GO present a favorable and often spontaneous self-limiting clinical course, although it may be prolonged over one or more years. Patients who suffer from severe forms of GO can be treated with systemic corticosteroids or orbital irradiation.

## Imaging Findings

Orbital MRI study demonstrates diffuse orbital fat involvement in both sides and fusiform thickening of the extraocular muscles with tendon sparing (Fig. 2.2a). On axial and coronal STIR sequence (Fig. 2.2b, c), the extraocular muscles present high signal intensity consistent with inflammatory component. Note the optic nerve encasement in the apex of the orbit due to muscles enlargement (*arrow* in Fig. 2.2b).



**Case 3****History****Inflammatory Pseudotumor of the Orbit**

A 28-year-old woman presented with a mass located in superolateral aspect of the left orbit of 6 months duration. The patient also complained of vague symptoms of tearing, limited motility of the left eye, and episodes of orbital inflammation since the last 2 weeks.

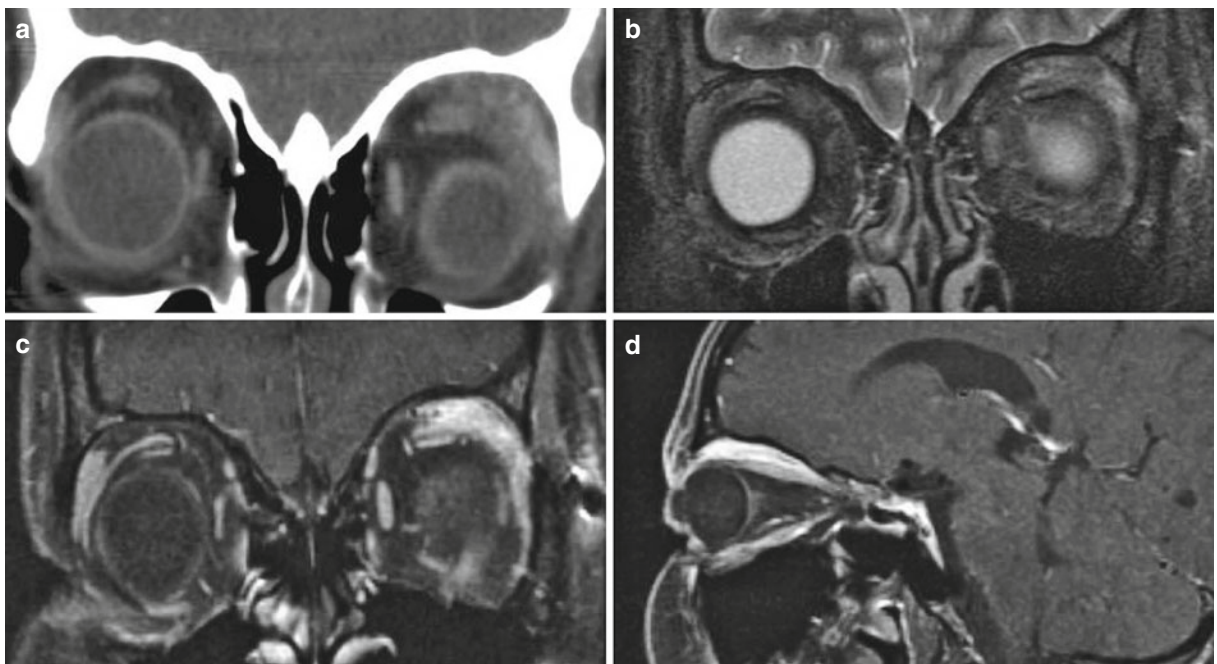


**Fig. 2.3**

An inflammatory pseudotumor of the orbit represents a clinical and pathologic condition of unknown etiology that is characterized by the presence of a mass within the orbit that may mimic malignancy and that is composed of inflammatory cells and variable amounts of fibrosis. It constitutes about 9% of all orbital mass lesions. Inflammatory pseudotumors are most often confined to the orbit and frequently involve the lacrimal gland and the muscular cone. The extension of the lesion beyond the orbit or even intracranially is quite rare but it may occur in cases of extensive and chronic orbital inflammation. Orbital pseudotumor has no gender or race predominance and can appear in individuals of any age, although it most frequently occurs in middle-aged patients. It is usually unilateral, and the presence of bilateral masses suggests an underlying systemic disease.

The symptoms of idiopathic pseudotumors depend on the inflammatory response (acute, subacute, or chronic) and the location of the inflammatory tissue. Clinical manifestations include exophthalmos, reduced ocular motility, diplopia, ptosis, and chemosis. In fact, inflammatory pseudotumors are a common cause of unilateral proptosis in adults.

The radiological findings in a pseudotumor are characterized by inflammatory changes in the different intraorbital components, such as the globe, the lacrimal glands, the extraocular muscles, the orbital fat, and the optic nerve. On CT, inflammatory pseudotumors appear as an abnormal intraorbital mass of soft-tissue density, which varies widely in shape, location, and size. The presence of bony changes, reflected by hyperostosis or erosion and sclerotic change, indicates a long-standing benign process. Inflammatory pseudotumors of the orbit are frequently accompanied by edema or fat infiltration. On MRI, the lesions are hypointense on both T1- and T2-weighted images (possibly related to the fibrotic changes) with strong enhancement after gadolinium administration. Fat suppression techniques clearly show intraorbital inflammation.

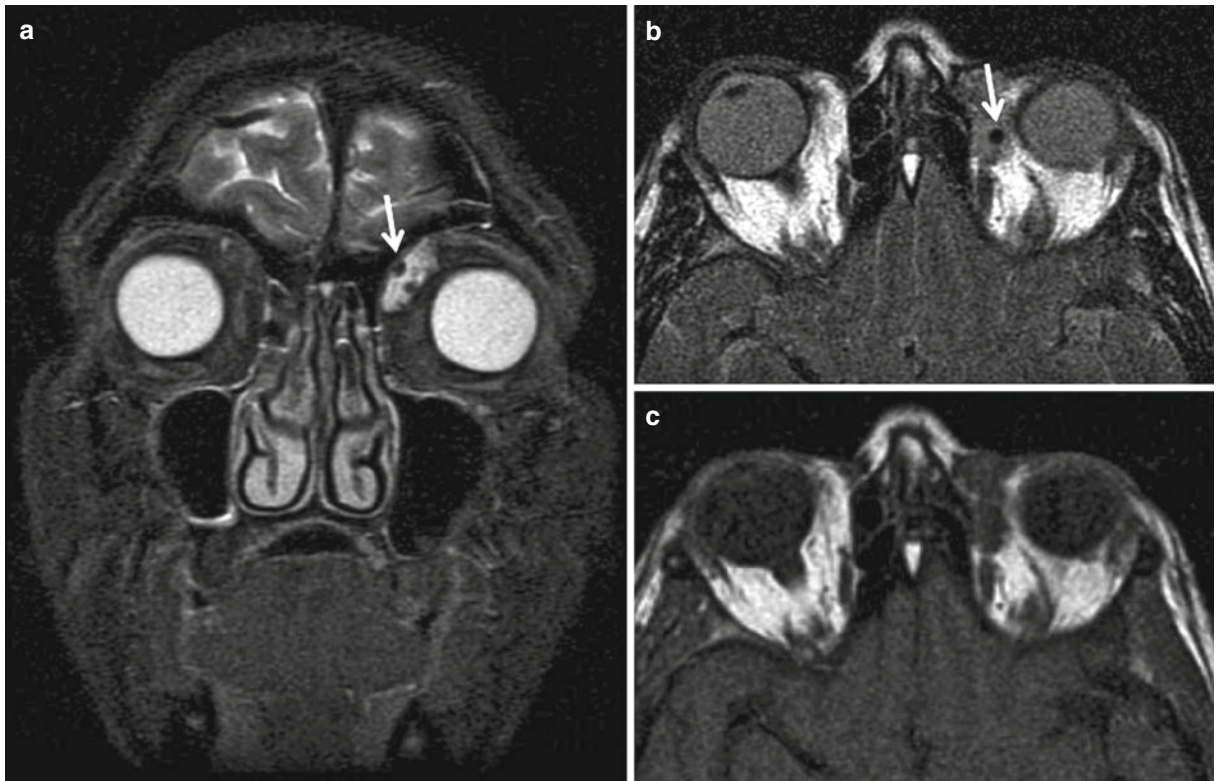
Orbital pseudotumor is diagnosed by exclusion, on the basis of the patient's history, clinical course, response to steroid therapy, laboratory test, and radiological and biopsy findings. The diagnosis becomes even more difficult in subacute and chronic forms. Sometimes, a chronic idiopathic inflammatory pseudotumor can simulate lymphoma, particularly when there is no history of an acute onset.

Corticosteroids are the mainstay of treatment and are administered for several months to ensure remission. Radiotherapy may be used in patients who fail to respond to steroids or who have a rapidly progressive course. For those patients who are refractory to both corticosteroids and radiotherapy, anecdotal reports have suggested the use of chemotherapeutic agents such as cyclophosphamide, methotrexate, and cyclosporine.

Orbital coronal CT scan (Fig. 2.3a) demonstrates an extraconal tumor in the theoretical location of left lacrimal gland. The tumor wraps around and displaces caudal and medially the ocular globe. On coronal STIR MR image (Fig. 2.3b), the lesion presents high signal intensity due to the inflammatory component. On coronal and sagittal gadolinium-enhanced fat-suppressed T1-weighted images (Fig. 2.3c, d), the tumor shows intense enhancement. Observe that the lesion is clearly depicted between orbital roof and superior rectus muscle in the sagittal plane.

## Comments

## Imaging Findings

**Case 4****Orbital Hemangioma****Fig. 2.4**



A 57-year-old woman presented with a soft mass located in superomedial portion of the left orbit that had been slowly growing for the last three years.

Cavernous hemangioma is the most common primary benign tumor of the orbit in adults. It is a slow-growing, vascular tumor, which is considered as developmental hamartoma. The tumor is characteristically unilateral and solitary; bilateral or multiple hemangiomas are quite rare. Most cavernous hemangiomas are located within the intraconal retrobulbar region. These tumors usually present in the fifth decade of life with female gender predominance. Pregnancy may accelerate the growth of the tumor.

The most common clinical presentation is a unilateral, painless, progressive proptosis. Other manifestations such as visual acuity compromise, diplopia, and extraocular muscle or pupillary dysfunction may occur as a result of compression of intraorbital contents by the tumor.

The diagnosis can be made by imaging studies. Ultrasound typically shows a lesion with good sound transmission with moderate high-echogenicity on A-scan secondary to the septae within the tumor. Doppler flow study may reveal subdued blood flow within the hemangioma. On CT scan, the tumor appears as an oval- or round-shaped, well-defined, homogeneous intraconal mass, which enhanced with intravenous contrast. The enhancing pattern can be homogenous or nonhomogenous. On MRI, hemangiomas are well-defined oval masses, homogeneous, isointense relative to muscle on T1-weighted images and hyperintense on T2-weighted images. On dynamic MRI after gadolinium administration, progressive and total homogeneous filling up of the mass can be seen. This enhancement pattern is considered a typical feature of a cavernous hemangioma of the orbit, and is similar to hepatic cavernous hemangiomas. The typical contrast-enhancement spread pattern of hemangiomas can be used to distinguish this tumor from others lesions such as schwannomas.

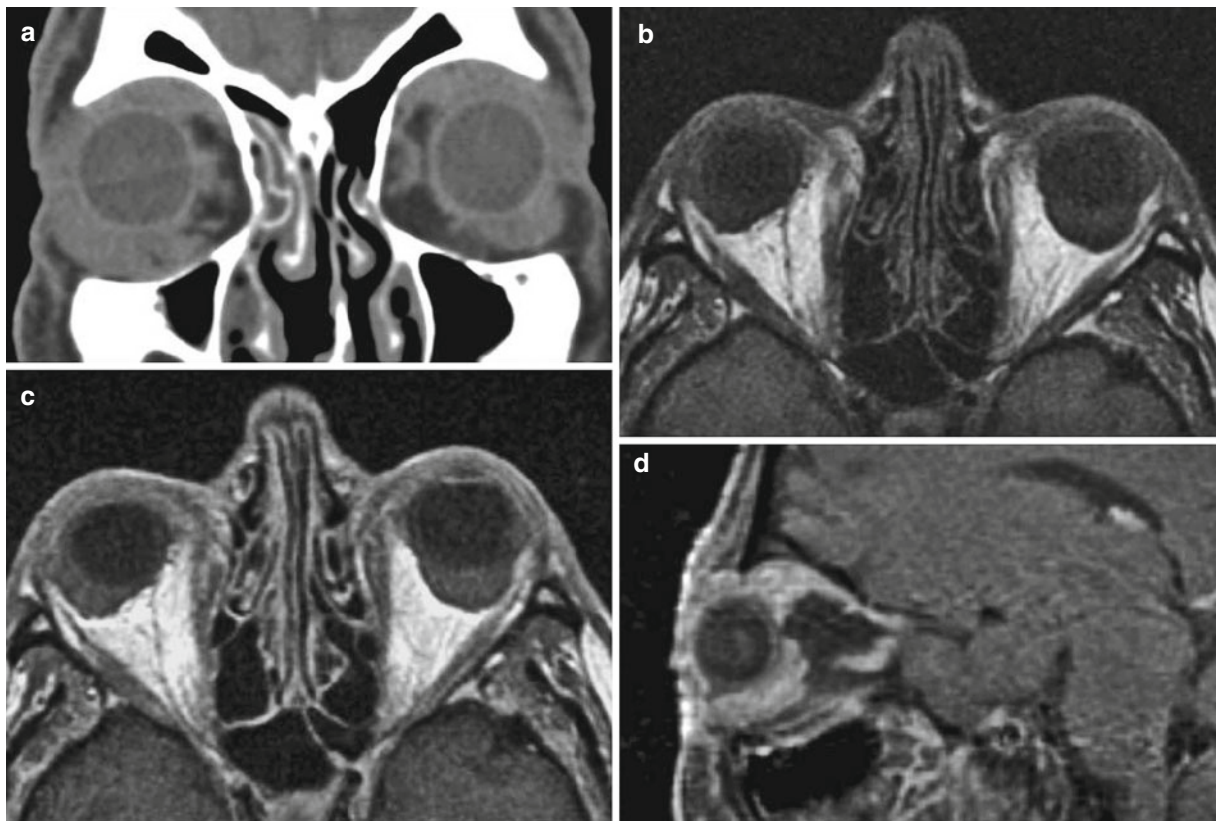
Most hemangiomas remain stable throughout a patient's life and cause no visual impairment, therefore, the majority of patients require no interventions and can be observed clinically. In cases of symptomatic tumors, surgical excision is the treatment of choice.

MRI study reveals a mass located in superomedial aspect of the left orbit, hyperintense on STIR (Fig. 2.4a), and T2-weighted (Fig. 2.4b) MR images and hypointense on T1-weighted image (Fig. 2.4c). The lesion presents well-defined lobulated margins and hypointense round images within it consistent with calcifications (pneolites) (*arrows*).

## History

## Comments

## Imaging Findings

**Case 5****Orbital Lymphoma****Fig. 2.5**

A 65-year-old male presented with bilateral eyelid swelling, moderate exophthalmos, and orbital discomfort.

## History

## Comments

Lymphomas are the most frequent orbital malignant tumors. According to recent publications, these tumors account for 11% of all orbital masses and 55% of all malignant tumors. Orbital lymphomas are predominantly low-grade, small, B-cell types, and are associated with systemic disease, occurring either sequentially or concurrently, in about one-third of the cases. Hence, a patient diagnosed with orbital lymphoma must be examined to rule out systemic disease. Normal orbital lymphoid tissue is located on conjunctivae and lacrimal glands, therefore, these are the most common locations of orbital lymphomas. Lymphoid tumors of the orbit are considered a disease spectrum that includes benign lymphoid hyperplasia, atypical lymphoid hyperplasia, and malignant lymphoma. There are no clinical or laboratory or imaging tests that permit to distinguish between benign and malignant lymphoid lesions.

Orbital lymphomas usually occur in older people, the average age for occurrence is the sixth decade of life and there is a slight female predominance. Clinically, lymphoma of the orbit generally presents with symptoms secondary to gradually increasing mass effect on surrounding structures. Clinical features include progressive painless proptosis with or without motility impairment, diplopia, ptosis, and, rarely, visual loss. Proptosis and visible conjunctival mass are the most common modes of presentation. Most lesions are unilateral although bilateral orbital involvement is seen in about 10–25% of the patients.

Ultrasound, CT, and MRI are different imaging techniques to diagnose orbital lymphoma. CT and MRI findings are unspecified and should be evaluated in conjunction with clinical signs and symptoms. On CT, orbital lymphomas appear as hyperdense, homogeneous well-defined masses usually located on the retrobulbar region or on the superior orbital compartment. The tumor is molded to the adjacent structures without eroding the bone or expanding the orbit. After contrast administration, the lesion shows mild enhancement. Biopsy is always mandatory for stage grouping of lymphomas. On MRI, malignant lymphoma lesions are hyperintense compared to the extraocular muscles on both precontrast and postcontrast T1-weighted images. When the lacrimal duct is involved or there is bilateral disease, it is more likely to be malignant lymphoma.

Therapeutic options for orbital lymphoma include surgical excision, radiation therapy, and chemotherapy. The prognosis depends on the histologic type and stage of lymphoma and therapy. In general, with modern treatment of patients with NHL, the overall survival rate at 5 years is approximately 60%.

Coronal un-enhanced CT-scan (Fig. 2.5a) demonstrates bilateral, solid, homogeneous, and soft-tissue attenuation masses that molded to the adjacent ocular globe. Lacrimal glands are involved and appear enlarged. On axial T1-weighted MR image (Fig. 2.5b), the lesions present the same signal intensity than extraocular muscles. On axial gadolinium-enhanced T1-WI (Fig. 2.5c) and sagittal contrast-enhanced fat-saturated T1-WI (Fig. 2.5d), the masses show homogeneous and intense enhancement.

## Imaging Findings

## Case 6

### Optic Nerve Sheath Meningioma

#### History

A 40-year-old female presented with progressive visual acuity loss in the left eye with self-limited episodes of mild ocular pain in this eye. On physical examination, slight proptosis and mild unilateral papilledema were found.

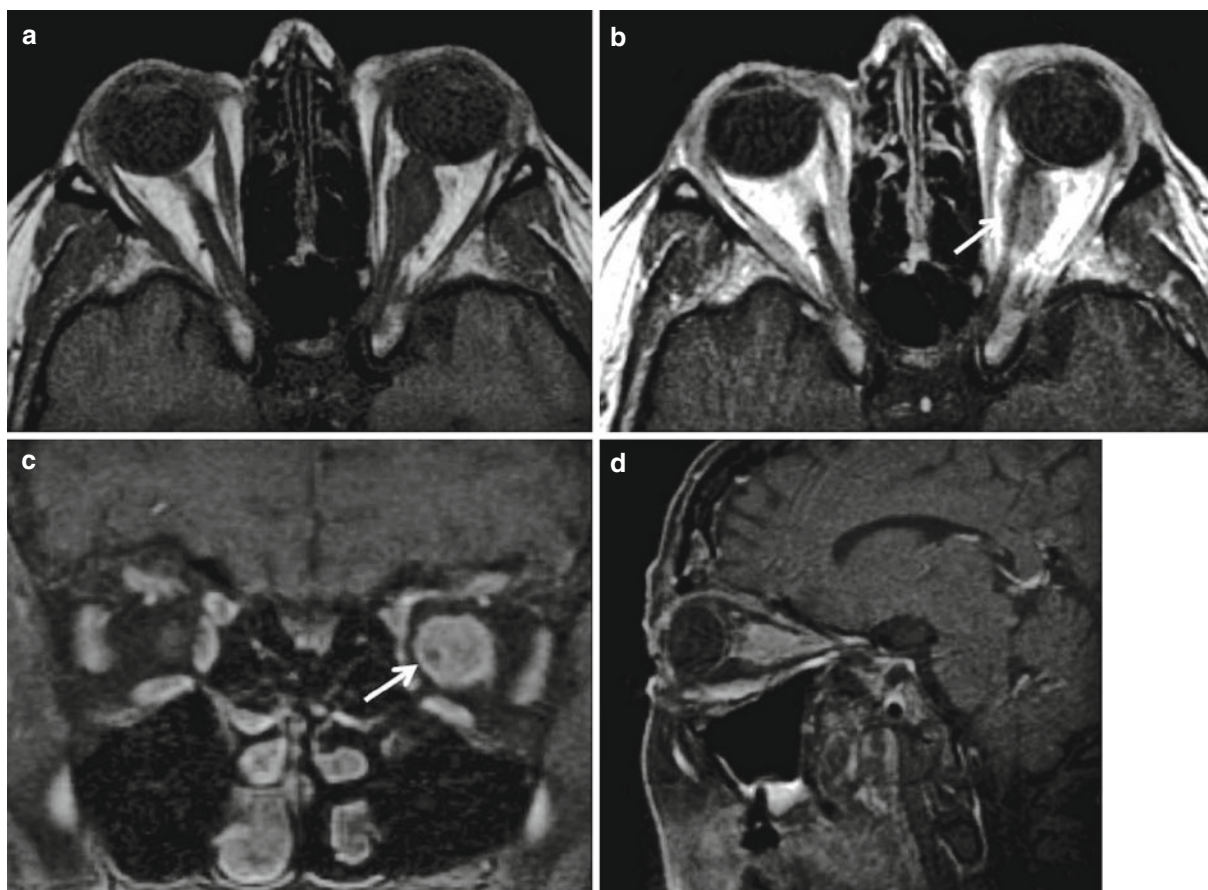


Fig. 2.6

Optic nerve sheath meningioma (ONSM) is a rare, benign tumor that arises from the cap cells of the arachnoid that surround the intraorbital or intracanalicular optic nerve. The tumor can develop anywhere along the course of the optic nerve. ONSM represents about 1–2% of all meningiomas, 2% of all orbital tumors, and about 10% of optic nerve lesions. The majority of cases occur in middle-aged females, with a 2:1 female-to-male ratio. The tumor may be unilateral, bilateral, or multifocal with the latter two subgroups occurring most commonly in patients with type 2 neurofibromatosis.

The clinical presentation of optic nerve sheath meningioma depends on whether they arise from the orbit, within the optic canal or intracranially. The tumor typically grows slowly causing gradually compression of the optic nerve with progressive visual loss in the affected eye. The classic triad, known as the Hoyt–Spencer triad, includes loss of vision, optic atrophy, and optociliary shunt vessels. These enlarged blood vessels indicated that the tumor has disrupted the natural circulation through the optic nerve to the retina and choroid. Other clinical manifestations are color vision disturbance, visual field defect, proptosis, optic disc edema, and motility impairment.

The diagnosis of ONSM relies heavily on imaging findings. MRI currently remains the method of choice for diagnosis of ONSM, although it is less sensitive than CT in the detection of calcification. ONSMs are typically isointense or slightly hypointense to brain and optic nerve tissue on T1-weighted images and hyperintense (may also be hypointense) on T2-weighted images. They present a homogeneous intense enhancement after gadolinium administration often suggesting in appearance a “tram track” around the hypointense optic nerve in axial sequences. Intracranial extension is rare and, when present, it is restricted in a short distance along the prechiasmatic optic nerve sheath. Contrast-enhanced CT is another useful imaging technique for evaluation of optic nerve sheath meningioma. On CT, the tumor usually appears as a fusiform thickening of the optic nerve. This enlargement may appear as localized or as an eccentric expansion of the optic nerve and occurs most commonly at the orbital apex. After intravenous contrast injection, ONSMs usually shows an intense homogeneous enhancement. Linear, diffuse, or patchy calcifications within or along an optic nerve mass are commonly detected.

The differential diagnosis includes optic glioma, orbital pseudotumor, and lymphoma.

ONSM management is variable and depends on several factors. In cases of mild or no visual impairment with evidence of no intracranial extension, follow-up is recommended. If loss of vision occurs and progresses, radiation therapy is the treatment of choice either primarily or following surgery. Radiotherapy can improve vision in some patients or preserve it in others. Chemotherapy is reserved for patients with unresectable, recurrent, or previously irradiated meningiomas.

Axial T1-weighted MR image of the orbits (Fig. 2.6a) demonstrates a fusiform lesion that surrounds the left optic nerve, isointense to extraocular muscles. After contrast material administration (Fig. 2.6c, d), the lesion shows intense and homogeneous enhancement. On both T1-weighted MR image (Fig. 2.6b) and contrast-enhanced fat-suppression T1-weighted MR images (Fig. 2.6c), the optic nerve can be clearly depicted. It appears thinner than contralateral optic nerve and encased by the lesion (*arrow* in Fig. 2.6c).

## Comments

## Imaging Findings



## Case 7

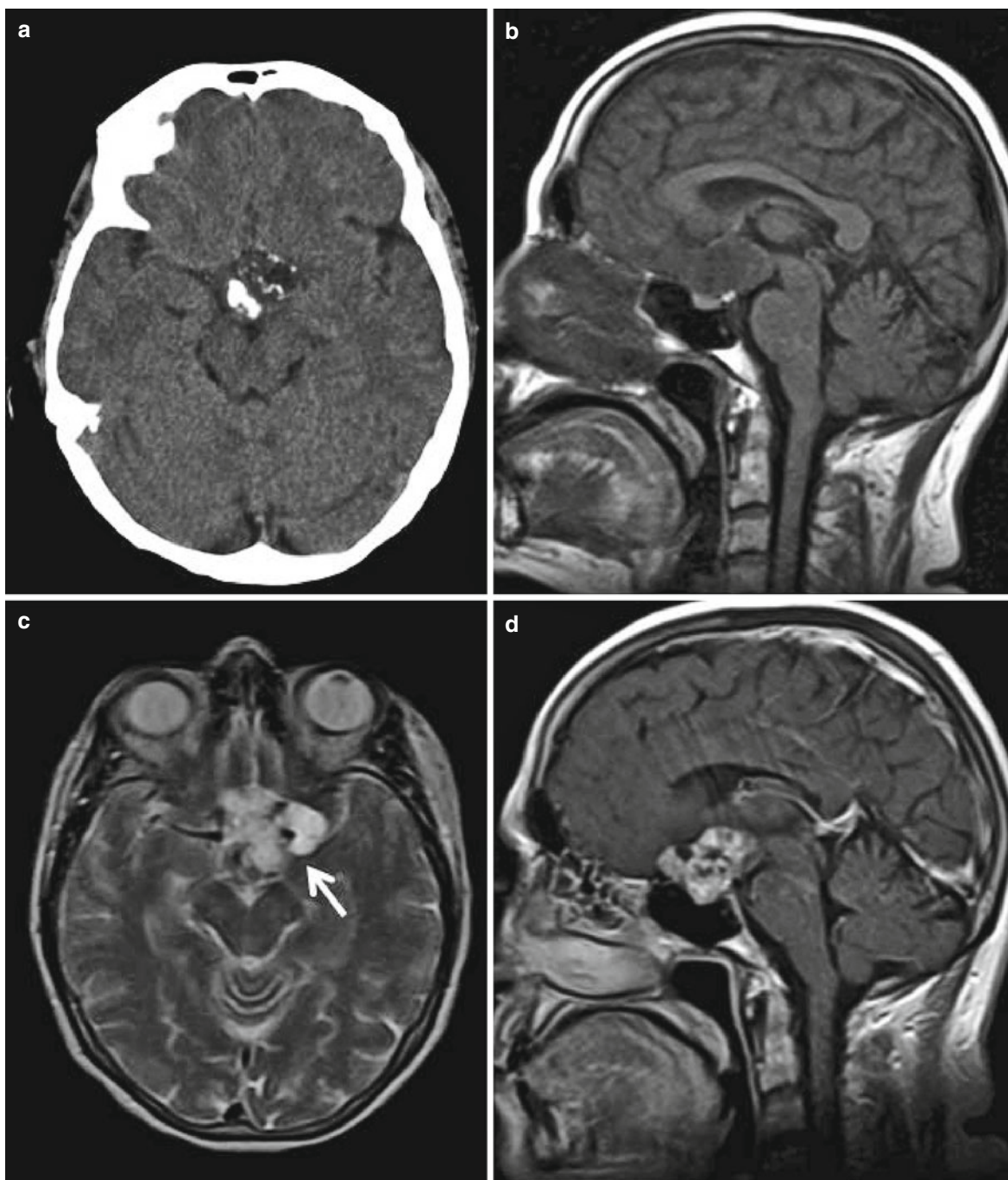
■  
Craniopharyngioma

Fig. 2.7

A 61-year-old woman was referred to ophthalmologist for visual loss and progressive headache. On physical examination, right temporal hemianopsia was found. Neuroimaging studies were performed next.

Craniopharyngioma is a benign, slow-growing, extra-axial, epithelial, calcified cystic tumor arising from squamous cell rests along the involuted hypophyseal Rathke's cleft. For this reason they occur exclusively in the region of the sella turcica and suprasellar cistern. Craniopharyngiomas account for 3–5% of all primary intracranial brain tumors. The prevalence of craniopharyngiomas peaks between 10 and 14 years of age, with a second peak occurring in the fourth to sixth decades of life. There is no gender predilection.

The most common presenting symptoms are headache, visual disturbances, and endocrine dysfunction. Although craniopharyngiomas exhibit no hormonal activity, endocrine symptoms can occur due to compression of the hypothalamus, pituitary stalk, and pituitary gland.

Imaging studies strongly suggest the diagnosis. The radiologic hallmark of a craniopharyngioma is the appearance of a suprasellar calcified and cystic mass. About 80–87% of craniopharyngiomas are calcified and 70–75% are cystic. Calcifications are more common in children (90%) than in adults (50%). CT scan is the most sensitive technique to demonstrate calcifications. It is useful in defining both calcified and cystic components. Cyst content usually has the same attenuation as cerebrospinal fluid (CSF); contrast administration better defines the enhancing cyst capsule. On MRI, craniopharyngiomas present a heterogeneous spectrum. The most common pattern is a cyst that is hypointense on T1WI and hyperintense on T2WI. Sometimes, craniopharyngiomas are hyperintense on T1WI due to high protein concentration, blood degradation products, or both. After gadolinium administration, the tumor enhances strongly and heterogeneously. MRI is the imaging modality used to plan the surgical approach.

Differential diagnosis includes the following entities: Rathke's cleft cyst, necrotic pituitary adenoma, suprasellar dermoid, teratoma, thrombosed aneurysm, and cystic suprasellar hypothalamic and chiasmatic glioma.

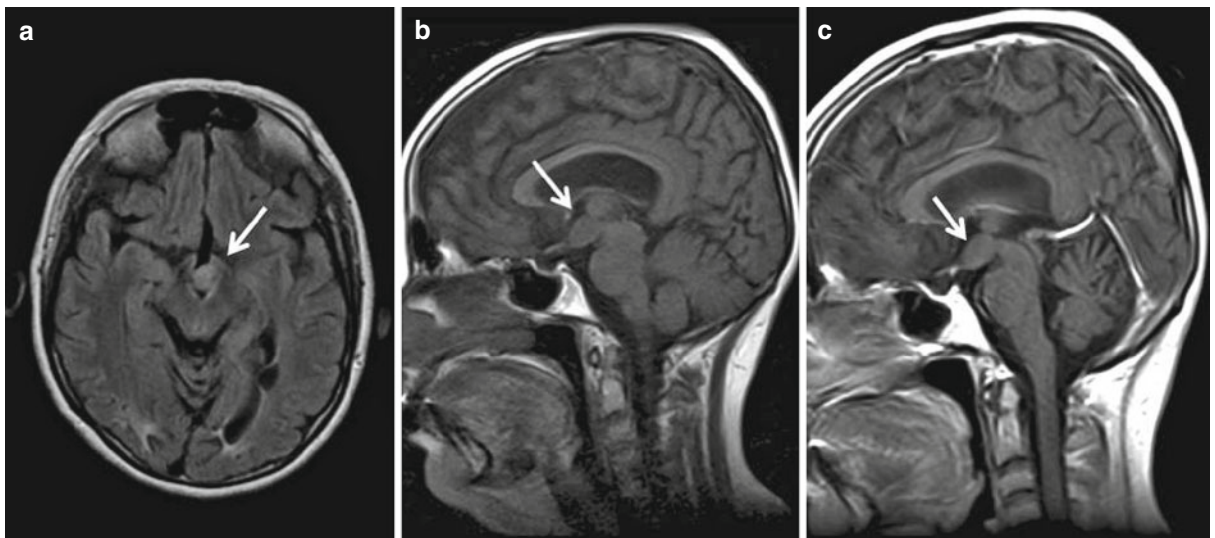
Surgical removal is the treatment of choice for tumor eradication. Nevertheless, craniopharyngiomas tend to recur after surgery. Therefore, postoperative follow-up with gadolinium-enhanced MRI is mandatory.

Un-enhanced CT scan (Fig. 2.7a) demonstrates a sellar and suprasellar mass, hypoattenuating to brain parenchyma, with calcifications. On MRI, the lesion appears hypointense on T1-weighted image (Fig. 2.7b) and hyperintense on T2-WI (Fig. 2.7c), which is consistent with a predominantly cystic component. After gadolinium administration (Fig. 2.7d), the tumor shows intense and heterogeneous enhancement and solid and necrotic or cystic components are better differentiated. Note encasement of left internal carotid artery by tumor (*arrow* in Fig. 2.7c).

## History

## Comments

## Imaging Findings

**Case 8****Hypothalamic Hamartoma****Fig. 2.8**

A 28-year-old woman underwent an urgent unenhanced CT-scan for cranial trauma after traffic accident. A small lesion located in interpeduncular cistern was incidentally found on CT. The patient referred a past medical history of epilepsy treatment long time ago.

Hypothalamic hamartoma, also called tuber cinereum hamartoma, is a relative rare congenital non-neoplastic heterotopia. It represents a midline dysraphic syndrome and presents as an ectopic cerebral gray matter, comprising a mass of normal neuronal tissue. Most of these lesions are small with a diameter of a few millimeters to 1.5 cm. They lie between the infundibular stalk anteriorly and the mamillary bodies posteriorly.

These lesions have been divided into two main clinicoanatomic types: para-hypothalamic hamartomas and intra-hypothalamic hamartomas. Parahypothalamic hamartomas are pedunculated masses that are attached to the floor of the hypothalamus by a narrow stalk. These lesions seem more likely to be associated with isosexual precocious puberty. Intrahypothalamic hamartomas are sessile masses with a broad attachment to the hypothalamus. These lesions seem to be associated more often with gelastic seizures, intellectual impairment, and psychiatric disturbances than with precocious puberty. These clinical features are noted commonly in early life and may occur as early as in the neonatal period.

On MR imaging, hamartomas appear as well-defined pedunculated or sessile lesions at the tuber cinereum and are isointense or mildly hypointense on T1-weighted images and iso- to hyperintense on T2-weighted images. Hamartomas neither calcify nor exhibit enhancement following contrast administration.

Surgery, radiosurgery, and medical treatment are the different therapeutic options. The choice of treatment must be individualized depending on the age and clinical circumstances of the patient and the size and anatomic relationships of the hamartoma.

The absence of any long-term change in the size, shape, or signal intensity of the lesion strongly supports the diagnosis of hypothalamic hamartoma.

Axial T1-weighted MR image (Fig. 2.8a) reveals a mass in interpeduncular cistern (*arrow*), isointense to brain parenchyma. Sagittal T1-weighted MR images, before (Fig. 2.8b) and after (Fig. 2.8c) intravenous gadolinium administration, show a lesion that lies between the infundibular stalk anteriorly and the mamillary bodies posteriorly (*arrows*). The mass presents the same signal intensity as the brain parenchyma and does not enhance with the contrast material.

## History

## Comments

## Imaging Findings



**History**  
**Case 9**  
**Pituitary**  
**Adenoma**  
**Comments**

A 18-year-old boy was referred to the emergency department with a three-day history of right periorbital headache, blurred vision, and diplopia. On physical examination, right temporal hemianopsia was found.

Pituitary adenomas are benign, slow-growing tumors that arise from cells in the pituitary gland. Pituitary adenomas are relatively common, accounting for approximately 15% of primary brain tumors. These tumors occur in individuals of 20–50 years of age and do not show gender predilection. Based on size, pituitary tumors can be divided into microadenomas (<1 cm in diameter) and macroadenomas (>1 cm in diameter). Microadenomas typically present with endocrine disturbances (according to the hormone secreted by the tumor),

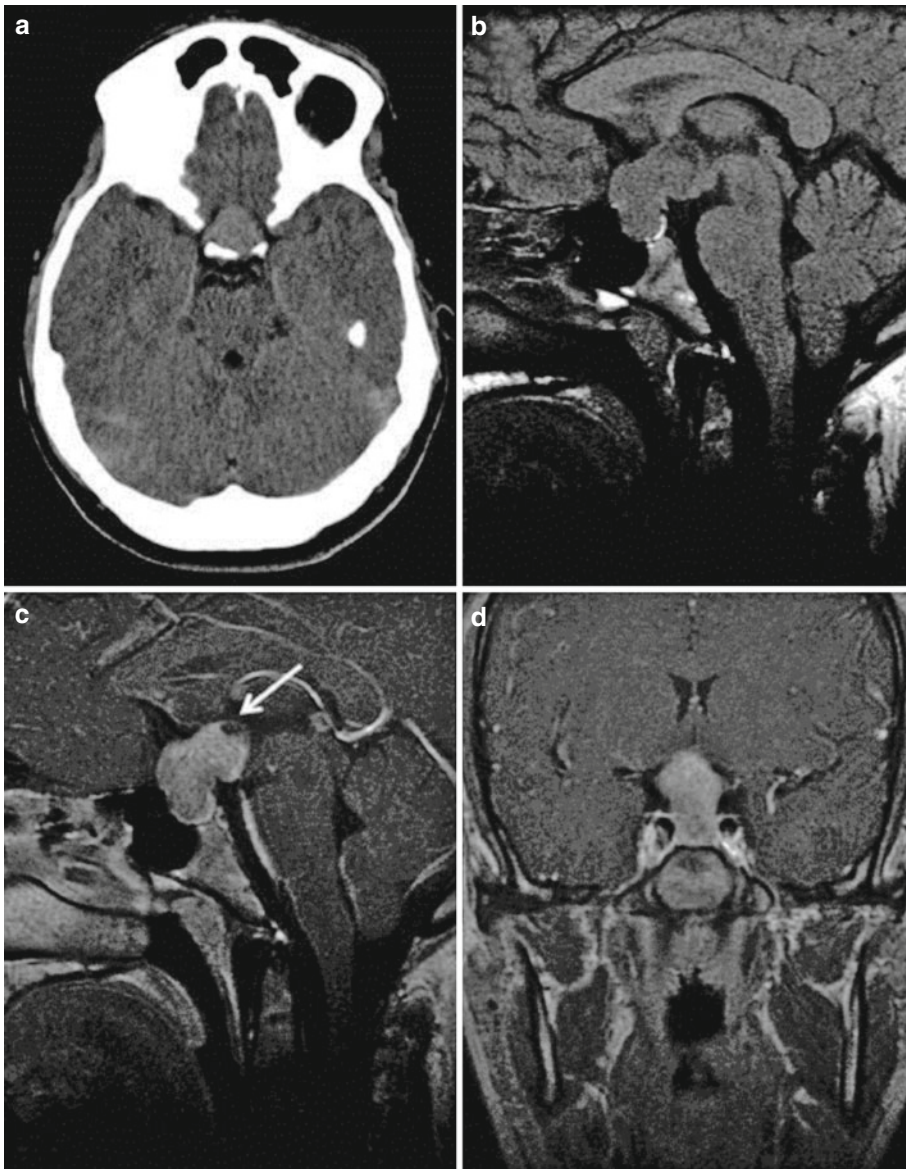


**Fig. 2.9**



whereas macroadenomas usually manifest with symptoms due to the local mass effect on the optic chiasm or with pituitary failure. Lateral extension of the tumor may involve cavernous sinus and may affect the III, IV, and VI cranial nerves causing ocular motility impairment.

Pituitary adenomas are usually solid capsulated tumors that may contain internal areas of necrosis, cyst formation, or hemorrhage. Calcifications are rare. According to the hormone secreted by the tumor, adenomas can be divided into two categories: (1) hormone-inactive (nonfunctional) pituitary adenomas, which typically cause problems related to the size of the tumor compressing adjacent brain structures and (2) hormone-producing pituitary adenomas. The three most common are prolactin-secreting pituitary adenoma (prolactinoma), growth hormone-secreting pituitary adenoma, and ACTH-secreting pituitary adenoma. Other hormone producing pituitary tumors are very rare. Pituitary adenomas, with a few exceptions, are not under the control of hypothalamic releasing factors.

Clinical manifestations are due to the local effect of the mass and distant endocrine manifestations that can affect a variety of organ systems.

The diagnosis of a pituitary adenoma is made based on a combination of pituitary function testing (blood hormone levels) and pituitary imaging. Conventional single-section CT has a limited role in pituitary imaging, with a sensitivity of 17–22% in detecting microadenomas. Multidetector-row CT with 64 channels may have a role, especially in patients unable to undergo MRI. CT is best for visualizing bony detail and calcification. On CT, microadenomas appear as a focal hypodense area within the pituitary gland. MRI is generally preferred over CT for the diagnosis of pituitary adenomas because of its superior definition of small lesions in the pituitary sella and its improved anatomic definition before surgery. MRI is also preferred for postsurgical surveillance. On MRI, microadenomas are sometimes difficult to detect unless dynamic techniques are used. Microadenomas enhance less rapidly than normal pituitary tissue and therefore appear relatively hypointense on rapid-sequence contrast-enhanced T1-WI. Uncomplicated macroadenomas show the same signal intensity than gray matter on all imaging sequences. Enhancement after gadolinium injection is typically intense but is often heterogeneous.

The optimal treatment of a pituitary adenoma depends on multiple factors including the hormone production by the tumor (if present), size of the tumor, how invasive the tumor is into surrounding structures, and the age and health of the patient. Treatment options include surgery (performed in more than 99% of cases via a transphenoidal route), radiotherapy, and medical treatment.

On urgent noncontrast CT scan (Fig. 2.9a), a sellar and suprasellar hyperattenuating mass was found. On MRI study, the lesion is well-circumscribed and appears isointense to brain parenchyma on T1-weighted image (Fig. 2.9b). After intravenous gadolinium administration (Fig. 2.9c,d), the mass shows intense and homogeneous enhancement. A small cystic component can be seen in the superior aspect of the lesion (*arrow* in Fig. 2.9c). The large suprasellar component of the tumor causes optic chiasm compression. This structure cannot be identified.

## Imaging Findings

## Case 10

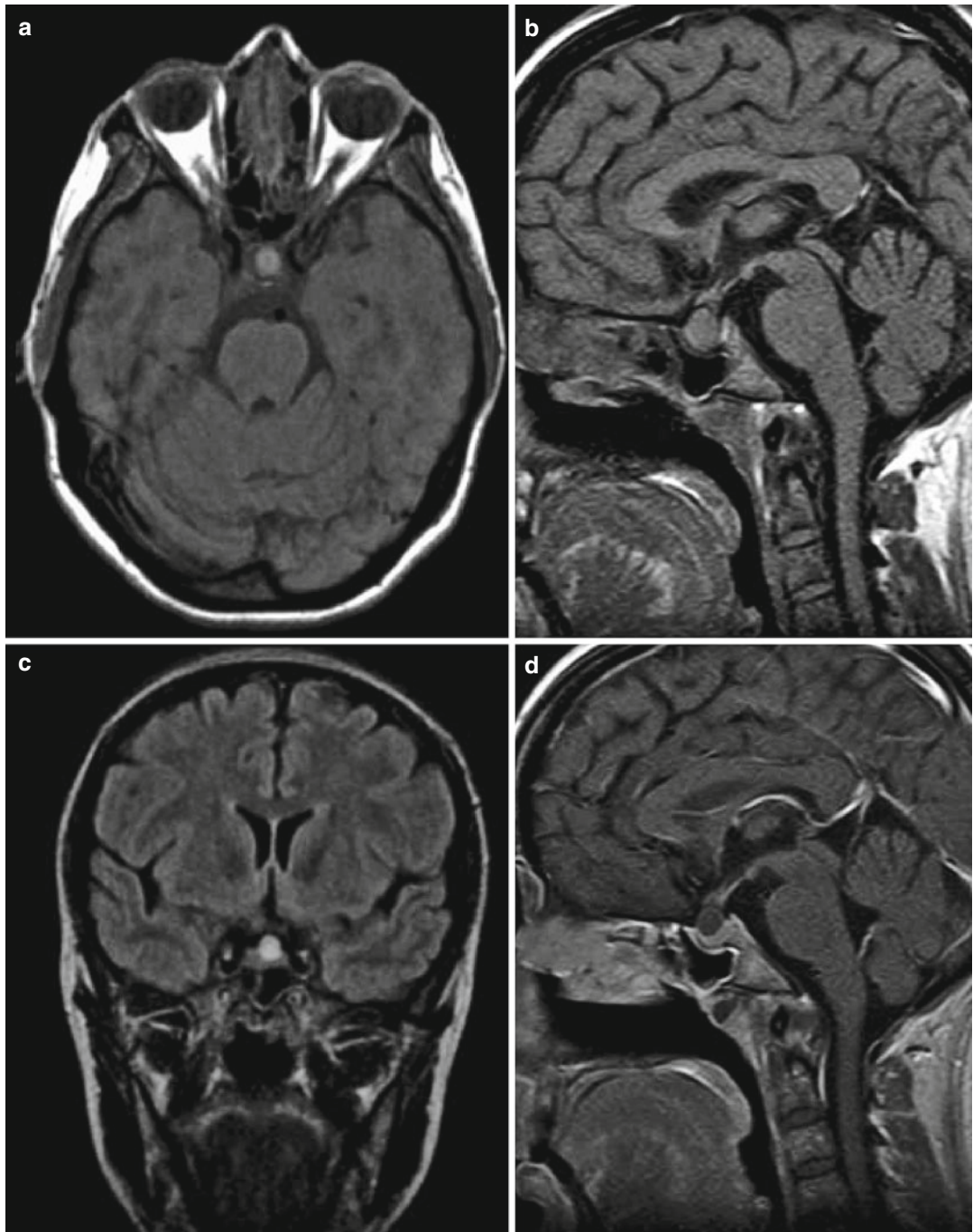
■  
Rathke's Cleft Cyst

Fig. 2.10

A 38-year-old woman presented with tension-type headache. She underwent a cerebral MRI study that demonstrated an “incidental” pituitary tumor.

Rathke’s cleft cysts (RCCs) are benign cystic lesions that originate from the failure of obliteration of lumen of the Rathke pouch. RCCs commonly appear as single, unilocated, well-defined, intra/suprasellar cyst without calcification. Forty percent of these cysts are completely intrasellar and the remaining 60% have suprasellar extension. They commonly measure between 5 and 15 mm but can occasionally become very large. Cyst contents vary from serous to mucoid. Most lesions are detected in middle-aged adults with female gender predominance.

The vast majority of RCCs are asymptomatic and they are found incidentally on imaging studies. Symptomatic RCCs are rare, but cysts can enlarge and produce symptoms as pituitary dysfunction, visual disturbances, and/or headache.

On CT, RCCs appear as well-delineated, round, hypodense, intra/suprasellar mass without enhancement after contrast administration. MRI findings depend on the cyst content. On T1-weighted image, two-thirds are hyperintense to brain and one-third show low signal intensity similar to CSF. On T2 WI, half are hyperintense, 25% are isointense, and 25% are hypointense. RCCs typically do not show enhancement following gadolinium administration, although an enhancing rim of compressed pituitary gland surrounding the cyst is sometimes present.

The differential diagnosis includes arachnoid cyst, cystic pituitary adenoma, cystic craniopharyngioma, and inflammatory cyst.

Asymptomatic RCCs are treated conservatively. In symptomatic cases, drainage or partial excision of the cyst wall (“marsupialization”) may be done. The recurrence rate varies from 19 to 28%.

Axial and sagittal T1-weighted MR images (Fig. 2.10a, b) and fluid-attenuated inversion recovery (FLAIR) MR image (Fig. 2.10c) reveal a hyperintense nodular lesion located in the pituitary gland. On sagittal contrast-enhanced T1-weighted MR image (Fig. 2.10d), the lesion does not show enhancement and can be clearly differentiated from hypophysis.

## History

## Comments

## Imaging Findings

## Further Reading

- Arita K, Ikawa F, Kurisu K et al (1999) The relationship between magnetic resonance imaging findings and clinical manifestations of hypothalamic hamartoma. *J Neurosurg* 91:212–222
- Augsburger JJ, Peyster RG, Markoe AM et al (1987) Computed tomography of posterior uveal melanomas. *Arch Ophthalmol* 105(11):1512–1516
- Barkovich AJ (2005) Intracranial, orbital, and neck masses of childhood. In: Barkovich AJ (ed) *Pediatric neuroimaging*, 4th edn. Lippincott Williams & Wilkins, Philadelphia, pp 573–603
- Bartalena L, Baldeschi L, Dickinson A, Eckstein A, Kendall-Taylor P, Marcocci C (2008) Consensus statement of the European Group on Graves' orbitopathy (EUGOGO) on management of GO. *Eur J Endocrinol* 158(3):273–285
- Bilaniuk L (1999) Orbital vascular lesions: role of imaging. *Radiol Clin North Am* 37:169–183
- Billeci D, Marton E, Tripodi M et al (2004) Symptomatic Rathke's cleft cysts: a radiological, surgical and pathological review. *Pituitary* 7(3):131–137
- Bonneville JF, Cattin F, Bonneville F (2009) Imaging of pituitary adenomas. *Presse Med* 38(1):84–91
- Boyko OB, Curnes JT, Oakes WJ, Burger PC (1991) Hamartomas of the tuber cinereum: CT, MR, and pathologic findings. *AJNR Am J Neuroradiol* 12:309–314
- Bunin GR, Surawicz TS, Witman PA et al (1998) The descriptive epidemiology of craniopharyngioma. *J Neurosurg* 89(4):547–551
- Cham MC, Pavlin CJ (2000) Ultrasound detection of posterior scleral bowing in young patients with choroidal melanoma. *Can J Ophthalmol* 35(5):263–266
- Chanson P, Salenave S (2004) Diagnosis and treatment of pituitary adenomas. *Minerva Endocrinol* 29(4):241–275
- Dodds NI, Atcha AW, Birchall D, Jackson A (2009) Use of high-resolution MRI of the optic nerve in Graves' ophthalmopathy. *Br J Radiol* 82(979):541–544
- Gupta DK, Ojha BK, Sarkar C, Mahapatra AK, Mehta VS (2006) Recurrence in craniopharyngiomas: analysis of clinical and histological features. *J Clin Neurosci* 13(4):438–442
- Hagiwara A, Inoue Y, Wakasa K et al (2003) Comparison of growth hormone-producing and non-growth hormone-producing pituitary adenomas: imaging characteristics and pathologic correlation. *Radiology* 228(2):533–538
- Harold Lee HB, Garrity JA, Cameron JD, Strianese D, Bonavolontà G, Patrinely JR (2008) Primary optic nerve sheath meningioma in children. *Surv Ophthalmol* 53(6):543–558
- Ing E, Abuhaleeqa K (2007) Graves' ophthalmopathy (thyroid-associated orbitopathy). *Clin Surg Ophthalmol* 25:386–392
- Jacobs D, Galetta S (2002) Diagnosis and management of orbital pseudotumor. *Curr Opin Ophthalmol* 13(6):347–351
- Jung WS, Ahn KJ, Park MR et al (2007) The radiological spectrum of orbital pathologies that involve the lacrimal gland and the lacrimal fossa. *Korean J Radiol* 8(4):336–342
- Lee EJ et al (2005) MR Imaging of orbital inflammatory pseudotumors with extraorbital extension. *Korean J Radiol* 6(2):82–88
- Mafee MF et al (2005) Anatomy and pathology of the eye: role of MR imaging and CT. *Neuroimaging Clin N Am* 15:23–47
- Meredith TA (1998) Choroidal melanoma: diagnosis and management. *Am J Ophthalmol* 125(6):865–867
- Nishioka H, Haraoka J, Izawa H, Ikeda Y (2006) Magnetic resonance imaging, clinical manifestations, and management of Rathke's cleft cyst. *Clin Endocrinol (Oxf)* 64(2):184–188
- Noth D, Gebauer M, Müller B et al (2001) Graves' ophthalmopathy: natural history and treatment outcomes. *Swiss Med Wkly* 131:603–609
- Ohtsuka K, Hashimoto M, Akiba H (1997) Serial dynamic magnetic resonance imaging of orbital cavernous hemangioma. *Am J Ophthalmol* 123:396–398
- Osborn A (1994) *Diagnostic neuroradiology*. Mosby, London, pp 649–654
- Park SB, Lee JH, Weon YC (2009) Imaging findings of head and neck inflammatory pseudotumor. *AJR Am J Roentgenol* 193(4):1180–1186; Review
- Rey-Porca C, Pérez-Encinas M, González F (2008) Orbital lymphomas. Presentation of nine cases. *Arch Soc Esp Oftalmol* 83(2):95–103
- Saeed P, Rootman J, Nugent RA, White VA, Mackenzie IR, Koornneef L (2003) Optic nerve sheath meningiomas. *Ophthalmology* 110(10):2019–2030
- Saeki N, Sunami K, Sugaya Y, Yamaura A (1999) MRI findings and clinical manifestations in Rathke's cleft cyst. *Acta Neurochir (Wien)* 141:1055–1061
- Sharma RR (1987) Hamartoma of the hypothalamus and tuber cinereum: a brief review of the literature. *J Postgrad Med* 33:1–13
- Sibony PA, Krauss HR, Kennerdell JS, Maroon JC, Slamovits TL (1984) Optic nerve sheath meningiomas. Clinical manifestations. *Ophthalmology* 91(11):1313–1326
- Som PM, Curtin HD (2003) *Head and neck imaging*, 4th edn. Mosby, St Louis, pp 329–330
- Tanaka A, Mihara F, Yoshiura T et al (2004) Differentiation of cavernous hemangioma from schwannoma of the orbit: a dynamic MRI study. *AJR* 183:1799–1804
- Thorn-Kany M, Arrue P, Delisle MB, Lacroix F, Lagarrigue J, Manelfe C (1999) Cavernous hemangiomas of the orbit: MR imaging. *J Neuroradiol* 26:79–86
- Tominaga JY, Higano S, Takahashi S (2003) Characteristics of Rathke's cleft cyst in MR imaging. *Magn Reson Med Sci* 2(1):1–8
- Turbin RE, Pokorny K (2004) Diagnosis and treatment of orbital optic nerve sheath meningioma. *Cancer Control* 11(5):334–341
- Weber AL, Romo LV, Sabates NR (1999) Pseudotumor of the orbit. Clinical, pathologic, and radiologic evaluation. *Radiol Clin North Am* 37:151–168
- Yadav BS, Sharma SC (2009) Orbital lymphoma: role of radiation. *Indian J Ophthalmol* 57(2):91–97

Learning Neuroimaging

100 Essential Cases

Bravo-Rodríguez, F. de A.; Diaz-Aguilera, R.; Hygino da Cruz Jr., L.C. (Eds.)

2012, XIV, 226 p. 100 illus., 21 illus. in color., Softcover

ISBN: 978-3-642-22998-5